Earth Planet. Sci. Lett. 685 (2026) 120025

Contents lists available at ScienceDirect

Earth and Planetary Science Letters

journal homepage: www.elsevier.com/locate/epsl

Seismicity modulation along the Aleutian arc volcanoes occurs over multiple time scales

B. Senapati *, K.I. Konstantinou

Department of Earth Sciences, National Central University, Zhongli 320, Taiwan

ARTICLE INFO

Editor: Dr C Carolina Lithgow-Bertelloni

Keywords:
Aleutian arc
Volcano seismicity
Seasonal modulation
Polar motion
Volcanic hazards

ABSTRACT

Establishing a causal link between external forcings and observed seismic or volcanic activity remains a key challenge. However, characterizing seismicity modulation in volcanic regions offers valuable insights into the interplay between geodynamic processes and external environmental forcings. In this study, we investigate possible links between external forcings and seismicity associated with eleven volcanoes located along the Aleutian arc considering multiyear (1989–2024) earthquake catalogs. Our findings suggest that climate-driven mass redistribution and rotational variations of the Earth influence the modulation of volcano seismicity. The observed seasonal seismicity modulation in the Katmai volcanic group correlates with snow depth variations, with peak seismicity occurring during the summer season. We also observe periodicities of 14-months at Augustine, Iliamna, Novarupta and Martin volcanoes and 6.4-years at Spurr and Redoubt volcanoes, both linked to centrifugal forces stemming from changes in the Earth's rotation rate and polar motion. Notably, no seismicity modulation is observed related to tides. Additionally, volcanic activity at Spurr and Redoubt occurs near the peaks of the polar radius, suggesting a link between rotational dynamics and eruption timing. We propose that stress changes in the crust due to periodic variation of hydrological loading and the Earth's rotational dynamics may influence earthquake timing, magnitude, and seismic energy release from volcanoes. This study also highlights the sensitivity of volcanoes to external forcings and provides insights into the dynamics of volcano seismicity, which contributes towards better assessment of volcanic hazards.

1. Introduction

Subduction zones are the most tectonically active regions on Earth, responsible for nearly 90% of global seismic activity and about 75% of explosive volcanic eruptions, thereby posing significant hazards to the people living near them (Syracuse and Abers, 2006). The seismic activity produced by volcanoes is significantly different from that generated by tectonic earthquakes. In most cases, volcanic eruptions are preceded by increased seismic activity beneath or near the volcanic edifice and are typically accompanied by seismic signals related to rock failure and fluid flow. Therefore, seismology has become an essential and reliable tool for monitoring volcanic systems and forecasting potential eruptions (McNutt and Roman, 2015).

The Aleutian arc is a prime example of an active subduction zone, formed by the subduction of the Pacific Plate beneath the North American Plate, generating intense seismicity and volcanism (Fig. 1). Volcanism along this arc is generally promoted by the steep subduction of the Pacific Plate and H_2O release from the downgoing slab (Buurman et al., 2014; Wei et al., 2021). This arc comprises a chain of 142 Quaternary volcanic centers, out of which 32 are active volcanoes as shown in Fig. 1, and have been monitored by the Alaska Volcano Observatory (AVO) seismic network since 1988 (Tibaldi and Bonali, 2017; Power et al., 2020). Most of these active volcanic centers are located along the eastern 2500 km of the arc, where the motion of the Pacific Plate is nearly perpendicular to the trench (Buurman et al., 2014). The eastern Aleutian arc also comprises two important volcanic groups, referred to as Katmai Volcanic Group (KVG) and the Cook Inlet Volcanic Group (CVG). The KVG is situated in the Katmai National Park about 440 km southwest of Anchorage and consists of a cluster of closely spaced stratovolcanoes and calderas (Tibaldi and Bonali, 2017). The major volcanoes of this group from south-west are Martin, Mageik, Novarupta, Trident and Katmai (Fig. 1). The last eruption in this region was the June 1912 VEI-6 Novarupta eruption, one of the most powerful volcanic events of the 20th century (Fierstein and Hildreth, 1992). Since then, this region has remained active by exhibiting gas emissions and the occurrence of seismicity without any eruption (Fig. S1). The CVG lies to

* Corresponding author at: Department of Earth Sciences, National Central University, Zhongli 320, Taiwan.
E-mail address: senapati.batakrusna@gmail.com (B. Senapati).

https://doi.org/10.1016/j.epsl.2026.120025
Received 31 December 2025; Received in revised form 12 March 2026; Accepted 29 March 2026

the northeast of the KVG and includes several glacier-covered strato-volcanoes such as Mount Redoubt, Mount Spurr, Iliamna, and Augustine Volcanoes (Fig. 1). These volcanoes are more active than KVG and have produced major eruptions in recent decades, notably the 1989–1990 and 2009 eruptions of Redoubt, 1992 eruption of Spurr and the 2006 eruption of Augustine (Fig. S2). Although the Aleutian Islands are sparsely populated, volcanic activity in the region poses significant risks to vital infrastructure, including oil industry facilities and trans-Pacific commercial aviation routes. Therefore, detailed analysis of the temporal variations in seismicity associated with these volcanoes and their associated driving mechanism can provide valuable insights into volcanic behavior and play a key role in improving eruption forecasting.

Identifying the connections between volcano seismicity and periodic external forcings could help to enhance the regional volcano hazard assessment. Previous studies have found a sensitivity of such forcings on various volcanoes worldwide such as Mount Etna (Lambert and Sottili, 2019; Sahoo et al., 2022), Kilauea, Hawaii (Dzurisin, 1980), Ruapehu, New Zealand (Girona et al., 2018), Mayon, Philippines (Jentzsch et al., 2001), the Axial seamount, United States (Wilcock, 2001; Sahoo et al., 2021), Campi Flegrei, Italy (Petrosino et al., 2018), Miyakejima, Japan (Kasahara et al., 2001) and Stromboli, Italy (Sottili and Palladino, 2012). These studies suggested that the external forcings perturb the stress field around volcanic or fault systems and potentially trigger or alter the seismic activity as well as influencing eruption timing (Wilcock, 2001; Petrosino et al., 2018; Senapati et al., 2022, 2023). For example, Wilcock (2001) and McNutt & Beavan (1987) suggested that seismicity associated with continental volcanoes and sea-floor hydrothermal systems such as Juan De Fuca ridge and Pavlof volcano can be modulated by solid Earth and Ocean tides. Sahoo et al. (2022) suggested that the eruption cycle and seismicity in the Mount Etna region could be triggered by rainfall induced stress changes. Lambeck (1980) proposed that centrifugal forces arising from the Earth's rotation rate and polar motion can deform the Earth's surface and trigger seismicity at seasonal to interannual timescales. The seismicity modulation by external forcings has also been confirmed experimentally by Boettcher and Marone (2004), considering creeping laboratory shear zones under normal stress vibrations. However, the effect of external forcings on earthquake occurrence at volcanic areas remains a debated issue.

In the present study, we explore the potential link between periodic external forcings, and seismicity associated with Aleutian arc volcanoes, using earthquake catalogs spanning >30 years. Our analysis begins with a detailed description of the earthquake catalogs and the selection of active volcanoes that exhibit sufficient and continuous events spanning several years. We then estimate the magnitude of completeness and apply declustering techniques to isolate independent seismic events. Subsequently, we search the periodicity patterns in the seismicity of each selected volcano and assess their correlation with stress variations induced by external forcings. Finally, we discuss the possible physical mechanisms driving the observed seismicity modulation and its effect on the seismic and volcanic activity before arriving at conclusions.

2. Data

2.1. Earthquake catalogs

The seismicity of the Alaska Peninsula and the Aleutian Islands volcanoes has been monitored by the Alaska Volcano Observatory (AVO) since 1988 (Power et al., 2020). Initially the AVO seismic

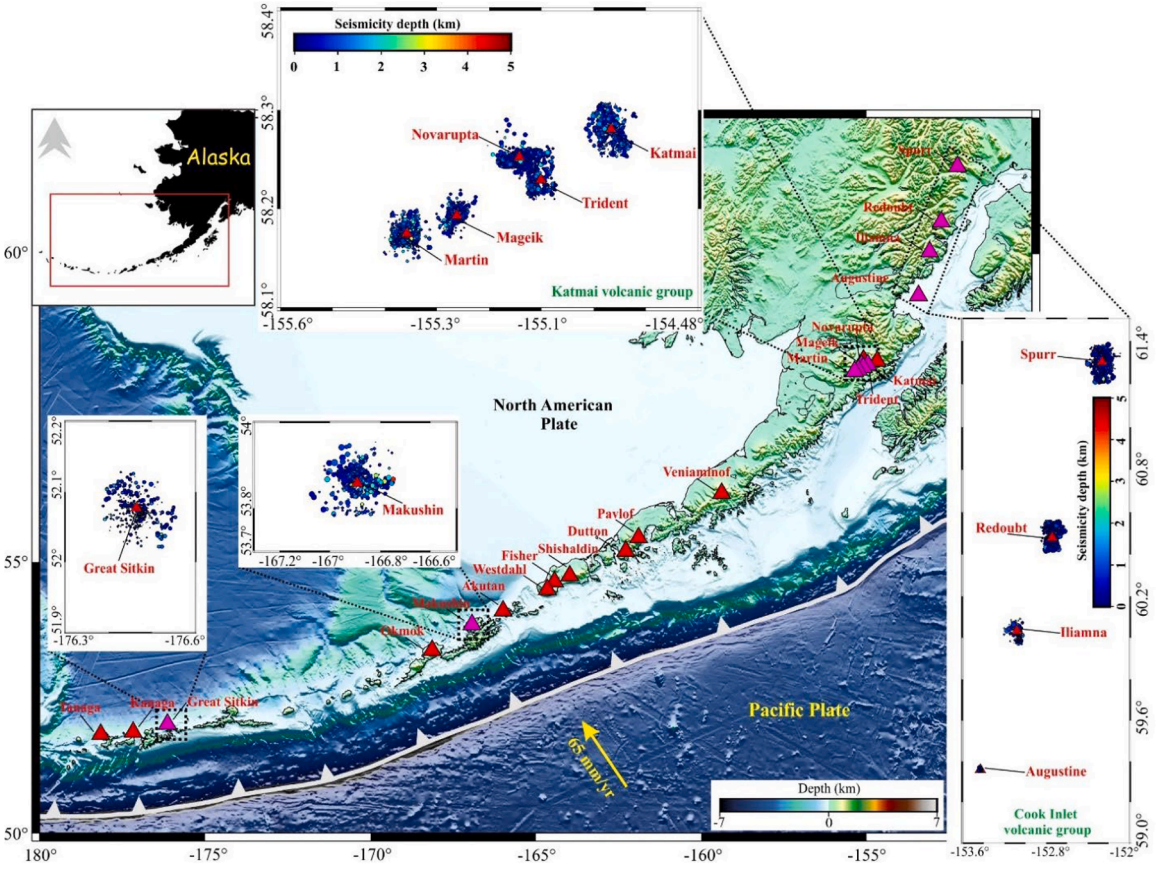

Fig. 1. General tectonics and bathymetry of the Aleutian trench along with the locations of the active volcanoes, represented by triangles. The active volcanoes considered in this study are represented by magenta triangles. Aleutian trench is marked by white line and the yellow arrow indicates the direction and motion of the Pacific plate with respect to North American plate, taken from Cross & Freymueller (2008). Insets represent the epicentral distribution of seismicity of the respective volcanoes.

network contained 29 stations and later expanded to 217 stations that provide real-time monitoring for 32 active volcanoes. As a result, AVO provides a long duration seismic catalog of >120,000 events consisting of volcano-tectonic, long-period and explosion signals, spanning from October 1989 to present time (Power et al., 2020). The volcanic seismicity generally occurs in a diffuse circular zone below the volcanic centers, hence we use a circle centered on the summit of each volcano to compile each catalog. The seismogenic depth and geographical extent of seismicity of each volcano are taken from Buurman et al. (2014) (see Table S1). The seismicity catalogs for the period of 1989 to 2017 are obtained from Power et al. (2019), while data for the period 2018–2024 are downloaded from the United States Geological Survey, online database. For the purpose of this study, we set three criteria in order to select the volcanoes that would be suitable for the investigation of seismicity modulation. The first criterion is that each selected volcano should exhibit significant volcano-tectonic seismicity (at least 2500 events). The second one requires that the recorded seismicity spans at least two decades or more, so that the long-term seismicity modulation can also be studied. The third criterion specifies that the volcano summit and its surrounding area must be seasonally covered with snow, so that the effect of snow loading on seismicity can be explored. Based on these criteria, eleven volcanoes were found along the Aleutian arc (Fig. 1 and Table S1), which are considered for further study.

2.2. Completeness magnitude

To determine statistically seasonal variations within seismicity catalogs, it is crucial to consider earthquakes only above the minimum magnitude of completeness (Mc). This requires an accurate assessment of Mc and its variations. Here, we apply the maximum curvature method as implemented by Woessner & Wiemer (2005) to estimate Mc for seismicity at each Aleutian arc volcano. This approach is based on the Gutenberg–Richter (GR) frequency–magnitude distribution, in which Mc corresponds to the point of maximum curvature in the non-cumulative magnitude histogram. The parameter Mc defines the lowest threshold magnitude above which the catalog is considered complete and minimally influenced by detection biases. The GR relationship can be expressed as (Gutenberg and Richter, 1944):

$$log_{10}N = a - bM(>Mc) \quad (1)$$

where N is the number of earthquakes with magnitude greater than Mc, a is a constant representing the overall level of seismicity. The slope of the GR relation, referred to as the b-value, represents the relative proportion between larger and smaller events in an earthquake population. The estimated Mc and b-values of the volcanoes are shown in Figure S3. Mc varies between 0.1 to 0.4 while the b-values vary between 0.94 ±0.047 and 1.44±0.063 (Fig. S3). The larger b-values are observed at Mageik, Augustine, Spurr and Great Sitkin indicating more heterogeneity as compared to other volcanoes (Fig. S3). The Mc and b-values estimated in this study are consistent with those reported by Konstantinou (2022), who applied the b-value stability method to determine Mc, thereby supporting the robustness of our findings.

2.3. Declustering procedure

Temporal clustering of seismicity can lead to statistical artefacts that resemble periodicity (Ader and Avouac, 2013). Seismicity catalogs often contain clusters of events such as foreshocks and aftershocks, that are triggered by a mainshock. These dependent events can cause biases in the periodicity pattern of seismicity, potentially amplifying or masking seismicity modulation. Therefore, a declustering procedure is crucial to isolate the background seismicity and to improve the reliability and interpretability of seismicity modulation by external forcings. Hence, to remove the densely clustered events in time and space, we declustered the seismicity catalogs using the growing cluster method of Reasenberg (1985) implemented in the Zmap package (Wiemer, 2001). The parametrization details are provided in the supporting information (Table S2). To further ensure the reliability of our declustering process, we additionally use the Nearest Neighbour algorithm to separate clustered seismicity from background seismicity (Zaliapin et al., 2008). This method evaluates the distribution of earthquakes by analyzing their occurrence times, spatial locations, and magnitudes to assess whether the seismicity displays clustering behavior or aligns with a random, background distribution. Notably, both declustering methods yielded a comparable number of events (Table S3).

3. External forcings and seismicity modulation

Seismicity can be influenced by various external forces that impose periodic stress perturbations on the lithosphere. These forcings include hydrological loading driven by seasonal snow and water mass redistribution, solid Earth and ocean tidal stresses, pole-tide effects from variations of the Earth's rotation axis, and longer-term changes associated with the Earth's rotational dynamics. Although the stress amplitudes generated by these processes are small compared to tectonic loading, they can become important when faults are close to failure (Perfettini et al., 2001; Heki, 2003; Craig et al., 2017). Such external stress variations are capable of modulating earthquake occurrence at seasonal, tidal, and multi-year timescales. In this study, we explore the influence of these external forcings on the seismicity associated with Aleutian arc volcanic centers.

3.1. Seasonal modulation

We use a spectral approach to search for the seasonal seismicity modulation of the Aleutian arc volcanoes considering declustered Mc catalogs. First, we generate a continuous seismicity time series by converting the entire period of the earthquakes into the number of events per hour. After that, the time-domain signal is transformed into the frequency domain using the Fast Fourier Transform method. From this analysis, we observe that the seismicity associated with KVG exhibits a strong annual and weak semi-annual periodicity, the CVG seismicity shows weak annual and seimi-annual periodicity, while Great Sitkin and Makushin volcanoes do not show any annual periodicity (Fig. 2). We also cross-check our results by performing the Schuster test following Ader & Avouac (2013) and notice that both results are consistent (Fig. S4 & S5). Further, the volcanoes along the Aleutian arc are covered with thick snow/ice, hence, in order to check whether the variation of snow thickness influences the seasonal seismicity modulation or not, we examine the correlation between the snow depth and declustered Mc seismicity. We observe a good correlation between occurrences of seismicity and timing of the seasonal snow loading (Fig. 3). The rate of seismicity occurrence in Katmai, Mageik, Novarupta and Trident volcanoes is increased during the summer season, in contrast to the seismicity rate associated with Martin volcano which decreases during the summer season (Fig. 3). We do not observe any clear relationship between the seismicity occurrence and snow thickness in the Great Sitkin and Makushin volcanoes (Fig. 3). To identify the time lags or leads between changes in snow depth and corresponding changes in earthquake activity, we also compute the lag cross-correlation between the declustered Mc seismicity and snow depth. From this systematic analysis, we find that the peak occurrence of seismicity has 2–3 months phase-lag relative to snow depth with cross-correlation coefficients of −0.35 to −0.76 except from Great Sitkin and Makushin volcanoes (Fig. 4).

We have also calculated the probability values (P_s) between the snow load induced stress and the seismicity of each volcano (Table 1). The vertical stress perturbation caused by the snow loading can be expressed as

$$\sigma_{zz} = \rho_s g h \quad (2)$$

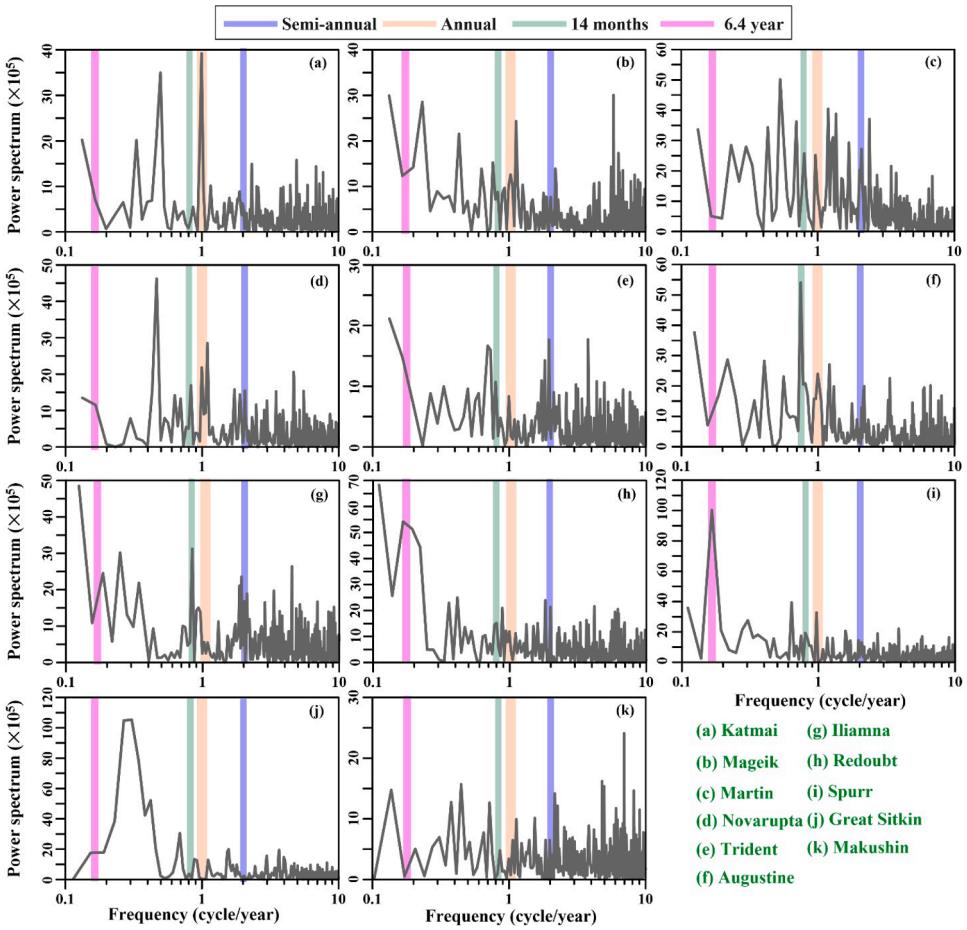

Fig. 2. Power spectra of declustered seismicity ($M \geq$ Mc) catalogs. Semi-annual, annual, pole tide (14-months) and pole wobble (6.4- year) periodicities are represented by the blue, peach, spring green and magenta color strips.

where σ_{zz} is the vertical stress change, ρ_s is the density of the snow, g is the acceleration due to gravity, and h is the thickness of the snow layer. In this study the density of snow is considered as 400 kg/m^3 (Ueda et al., 2024) and the acceleration due to gravity as 9.81 m/s^2. After the calculation of snow load induced stress over time, we determine the phase angle of each earthquake with respect to this induced stress which can take values from 0° to 360°, where 0° (or 360°) represents the peak and 180° represents the trough of the snow load induced stress (Fig. S6). Then, we calculate the probability P_s which is expressed as (Wilcock, 2001; Tang et al., 2019)

$$P_s = e^{(-R^2/m)} \tag{3}$$

where the parameter R is defined as

$$R = \sqrt{\left(\sum_{i=1}^{m} \sin\theta_i\right)^2 + \left(\sum_{i=1}^{m} \cos\theta_i\right)^2} \tag{4}$$

where θ_i is the phase angle of the i^{th} event and m is the total number of earthquakes. This statistical framework is based on the Rayleigh test (Trauth, 2007) for evaluating the non-uniformity of earthquake phase distributions on a circular scale. The test evaluates whether earthquake phases are randomly distributed or show significant clustering. The null hypothesis assumes that earthquake phases are uniformly distributed with no preferred alignment with periodic stress. The alternative hypothesis implies earthquake phases are non-uniform and show statistically significant clustering at particular phases of the stress cycle. Phase clustering was considered statistically significant when $P_s < 0.05$ corresponding to the 95% confidence level. In such cases, the null hypothesis of uniformity is rejected, and we may conclude that the correlation between earthquake occurrence and stress variations is unlikely to arise from random timing. This also implies that a lower probability (P_s) value indicates a stronger correlation between the earthquakes and stress variation (Tang et al., 2019). The estimated probability (P_s) values for the Aleutian arc volcanoes considered in the present study are shown in Figure S7 and Table 1. From this analysis, we observe that volcanoes in KVG have lower P_s values as compared to other volcanoes (Fig. S7 and Table 1). This indicates that the snow load induced stress influences the seasonal modulation observed in KVG.

The seismicity associated with KVG exhibits 2–3 months' phase lag with hydrological loading (i.e. snow depth, Fig. 4). This phase-lag may reflect the period required for fluids to migrate from the surface to seismogenic depths. To quantify this process, we estimate the crustal diffusivity by considering a simple one-dimensional fluid diffusion process (Saar and Manga, 2003), where the diffusivity (φ) is a function of seismogenic depth (d), phase-lag (γ) and period of the forcing (T) and can be expressed as (Saar and Manga, 2003)

$$\varphi = \frac{Td^2}{4\pi\gamma^2} \tag{5}$$

Considering the seismogenic depth and the phase-lag of the respective volcanoes exhibiting annual periodicity (Fig. 2), we estimate crustal diffusivities of ~0.16±0.03–0.84±0.07 m^2/s for Katmai, Trident, Novarupta, and Augustine while Martin and Spurr exhibit comparatively higher values, exceeding 1 m^2/s (Table 2). The estimated diffusivity range indicates highly fractured rock and is also similar to the previously estimated diffusivity for hydrologically induced seismicity

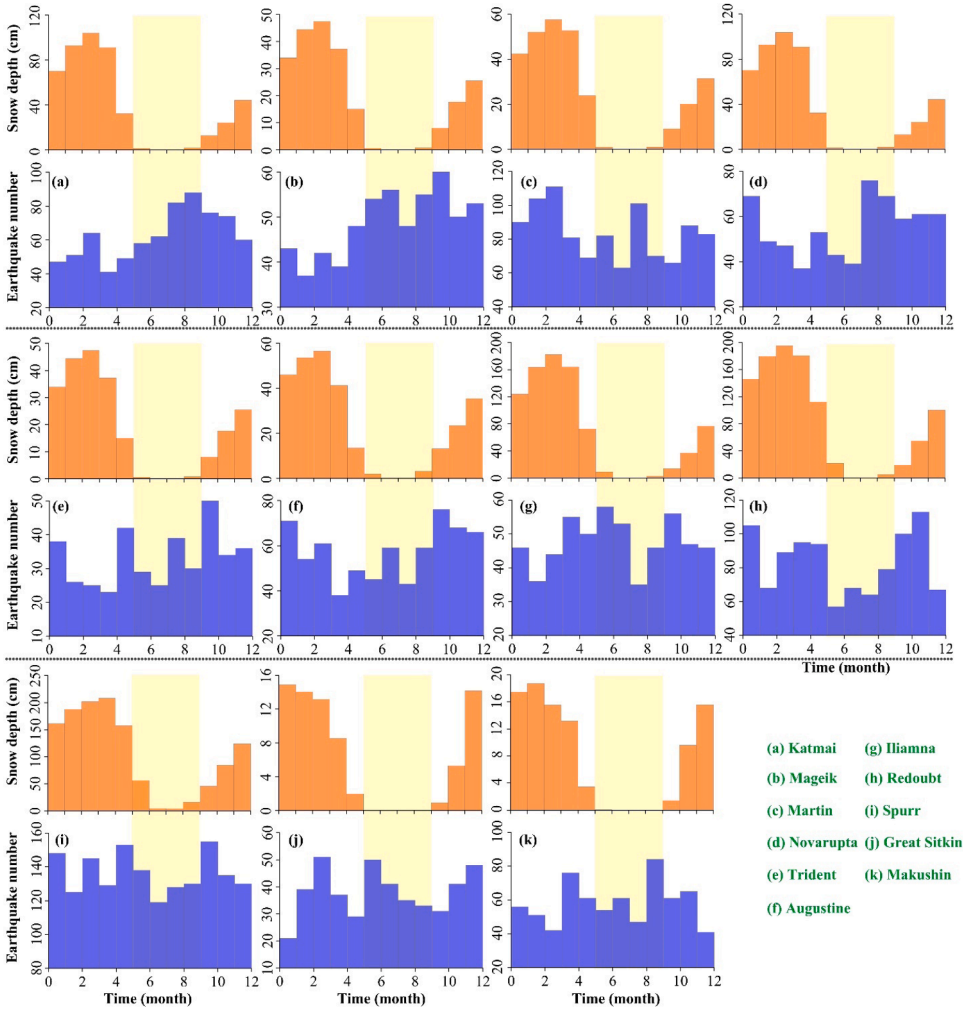

Fig. 3. Monthly histograms of snow depth and declustered seismicity ($M \geq$ Mc) observed at Aleutian arc volcanoes. The yellow strip indicates the unloading period (summer season). Note that the rate of seismicity increases during the summer season in contrast to the winter season in most of the volcanoes (see text for more details).

(Saar and Manga, 2003; Talwani et al., 2007). Further, we also estimate the permeability of the crustal zone between the seismicity and the surface. The permeability (K) is a function of the specific storage (α), dynamic viscosity (ϑ), distance for fluid migration (L) and the phase-lag between the seismicity and hydrological loading (γ) and is expressed as (Townend and Zoback, 2000)

$$K = \frac{\alpha \vartheta L^2}{\gamma} \tag{6}$$

Assuming α=10^{-10} Pa^{-1} and ϑ=10^{-4} Pa s (Nakajima and Uchida, 2018), we estimate that the permeability is between 7.71 × 10^{-15}±5.01 × 10^{-15} - 1.28 × 10^{-13} ± 5.7 × 10^{-13} m^2 (Table 2). Based on the estimated crustal diffusivity and permeability values, we infer that the observed phase lag between seismicity and hydrological loading at Katmai, Novarupta, Trident, and Augustine is consistent with pore-pressure diffusion, whereby elevated pore fluid pressure reduces effective normal stress and may possibly be modulating seismicity. In contrast, the higher diffusivity at Martin and Spurr, along with the negligible phase lag at Mageik cannot be explained by pore-pressure diffusion. Instead, seismicity in these systems is more likely modulated by the direct elastic stress associated with hydrological loading. These results are broadly comparable with the study of Saar and Manga (2003), where hydrologically modulated seismicity at Mt. Hood, Oregon occurs at depths of ~4.5 km with an inferred hydraulic diffusivity of ~0.3 ± 0.22 m^2/s and permeability on the order of ~10^{-15} m^2. The diffusivity values estimated in our study at depths of 2–3 km (~0.16–0.84 m^2/s) fall within a similar range, while the lower bound of our permeability estimates is also comparable to their results, suggesting similar hydrogeologic conditions that facilitate pore-pressure diffusion in fractured volcanic crust.

3.2. Pole-tide modulation

We also observe ~14-month periodicity in the seismicity associated with some of the Aleutian arc volcanoes including Augustine, Iliamna, Novarupta and Martin (Fig. 2). This periodicity exactly matches the oscillation period of the Earth's polar motion that is associated with the planet's ellipticity and is generally called the Earth pole tides. Pole tides are long-period deformations induced by the motion of the Earth's rotational axis relative to its crust, primarily governed by the ~14-month Chandler wobble (Gross, 2000). Although the amplitude of the crustal deformation induced by pole tides is very small (in the order of few millimeters to centimeters), it may influence the timing of earthquake occurrence in critically stressed regions. In order to investigate whether the ~14-month periodicity is caused by the pole tide induced stress, we have estimated the phase angle of each earthquake and P_s values following the same approach as in Section 3.1. First, we downloaded the polar motion data from the International Earth Rotation and Reference System Service Earth Orientation Center (IERS) online database. The rotation pole is measured along the x (Greenwich meridian)

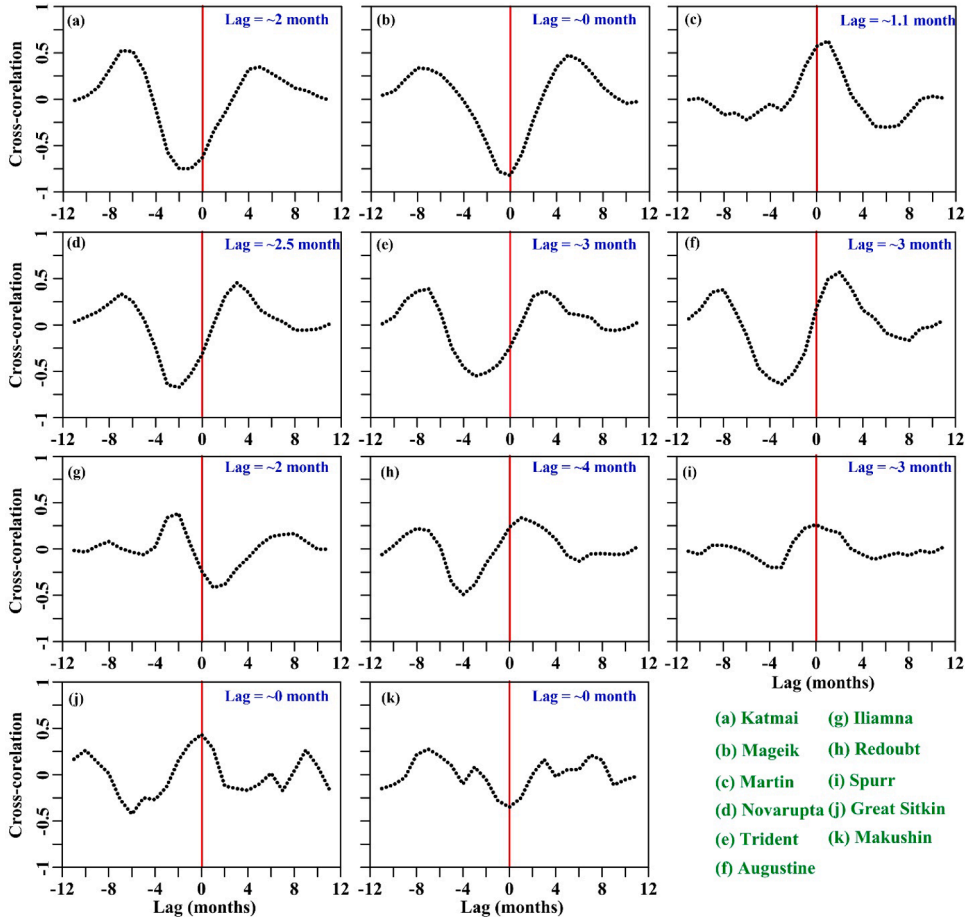

Fig. 4. Cross correlation-coefficient as a function of time lag between the declustered seismicity and snow depth for the volcanoes under study.

Table 1
P_s values for seismicity associated with volcanoes located along the Aleutian trench by considering snow load induced stress, pole-tide induced stress and total tidal stress (i.e., Ocean tide +Solid Earth Tide) respectively. P_s values < 0.05 are shown in bold fonts.

Name of Volcanoes	P_s values for snow load induced stress	P_s values for pole-tide induced stress		P_s values for tidal induced stress	
		Meridional stress	Radial shear stress	Horizontal stress	Shear stress
Katmai	**2.7×10^{-10}**	0.058	0.087	0.55	0.84
Mageik	**9.5×10^{-4}**	0.3	0.49	0.83	0.89
Martin	**5.3×10^{-5}**	**2.1×10^{-5}**	**8.8×10^{-8}**	0.28	0.37
Novarupta	**3.2×10^{-7}**	**1.2×10^{-3}**	**1.1×10^{-2}**	0.11	0.26
Trident	**2.5×10^{-3}**	**0.042**	**0.032**	0.15	0.30
Augustine	**7.7×10^{-6}**	**4.35×10^{-8}**	**1.5×10^{-7}**	0.95	0.86
Iliamna	0.64	**1.6×10^{-3}**	**1.9×10^{-3}**	0.97	0.73
Redoubt	**8.2×10^{-5}**	0.32	0.22	0.09	0.13
Spurr	**6.8×10^{-3}**	0.18	0.19	**0.01**	**0.02**
Great Sitkin	**0.023**	0.09	0.41	0.37	0.63
Makushin	**0.041**	0.35	0.39	0.54	0.78

Table 2
Quantitative estimation of crustal diffusivity and permeability for the volcanoes exhibiting seasonal modulation of seismicity due to snow load. Note that the uncertainty is estimated by fitting a Gaussian to the peak and the standard deviation of the fitted Gaussian represents the lag-time error. Uncertainties for diffusivity and permeability are estimated using error propagation based on the sensitivity of each parameter to the measured phase lag.

Name of Volcanoes	Depth of seismicity (km)	Time Lag (month)	Diffusivity (m^2/s)	Permeability (m^2)
Katmai	3	2 ± 1.23	0.84 ± 0.07	$1.7 \times 10^{-14} \pm 9.5 \times 10^{-15}$
Mageik	3	0 ± 1.48	——	——
Martin	3	1.1 ± 1.3	2.7 ± 0.3	$6.94 \times 10^{-14} \pm 1.8 \times 10^{-13}$
Novarupta	3	2.5 ± 1.4	0.53 ± 0.05	$1.3 \times 10^{-14} \pm 7.4 \times 10^{-15}$
Trident	3	3 ± 1.24	0.37 ± 0.04	$1.1 \times 10^{-14} \pm 5.1 \times 10^{-15}$
Augustine	2	3 ± 1.23	0.16 ± 0.03	$5.15 \times 10^{-15} \pm 4.01 \times 10^{-15}$
Spurr	10	3 ± 1.4	4.15 ± 0.45	$1.28 \times 10^{-13} \pm 5.7 \times 10^{-14}$

and y (90° east) axes of the terrestrial reference frame, respectively. This data has been recorded by means of optical measurements since 1846 and by various space and geodetic techniques (very long baseline interferometry, laser ranging to artificial satellites, global navigation satellite system, and Doppler orbitography by radio positioning integrated on satellite) since 1960. The accuracy of the data has drastically improved from several tens of milliarc second (mas) to <0.1 mas after the 1990s (Bizouard et al., 2019). In this study we use EOP C01 series of the Earth orientation parameters data, sampled at 0.05 years and available since 1900 to present date. After that, we calculate the pole tide-induced stress at the center of each volcano following Shen

et al. (2005) (for details see supporting information). The estimated meridional, zonal and radial shear pole tide-induced stresses are shown in Figure S8. From this analysis, we observe that P_s values are lower than 0.05 (95% confidence level) for seismicity associated with Augustine, Iliamna, Novarupta and Martin volcanoes (Figs. S9, S10 and Table 1). This suggests that the observed ~14-month periodicity is probably caused by the pole tide-induced stress perturbations. We also notice that the peak seismicity occurred during the ascension or close to the maximum pole-tide induced stress, suggesting that the timing of stress loading plays a crucial role in earthquake triggering (Figs. S9, S10).

3.3. Interannual pole wobble modulation

We also identify a 6.4-year periodicity in the seismicity associated with Spurr and Redoubt volcanoes (Fig. 2). This periodicity closely matches the retrograde oscillations of polar motion with a beating period of 6.4 years and arises from the continuous climate-driven excitation of the Earth's free rotational mode due to its ellipticity (Gross, 2000). Hence, we explore the relationship between polar motion amplitudes (pole radius), volcanic seismicity, and seismic energy by adopting the framework proposed by Lambert and Sottili (2019). The amplitude of the modulation of pole radius is proportional to the vertical displacement produced due to the variation of centrifugal force associated with the Chandler wobble and can be expressed as (Petit and Luzum, 2010)

$$PR = \sqrt{m_1 + m_2} \tag{7}$$

where m_1 and m_2 are the detrend vector components of m_x and m_y of rotational pole change, which are downloaded from the IERS online database.

We also calculate the seismic energy release at Spurr and Redoubt volcanoes defined as (Alparone et al., 2015)

$$log_{10}E = 9.9 + 1.9ML - 0.024ML^2 \tag{8}$$

where E is the seismic energy in Joule and ML is the local magnitude of earthquakes. To explore the link between the pole radius, seismic energy and volcanic activity, we calculate the monthly mean pole radius (PR) and seismic energy to obtain two continuous, evenly spaced time series shown in Fig. 5. Volcanic activity was then projected onto the polar radius plot, revealing that both eruptive, unrest periods (i.e. prolonged episodes that consist of several phenomena such as increased seismicity, ground deformation, hydrothermal or fumarolic activity changes and thermal anomalies etc.) and non-eruptive events (i.e. short-duration isolated episodes of increased seismicity, steam emissions, and fumarolic or hydrothermal activity etc.) at Spurr and Redoubt both occur near the peaks of the polar radius (Fig. 5b). This suggests a synchronous response of these volcanic systems to variations in the Earth's rotation rate and polar motion. Fig. 6a and 6e represent the variation of seismic energy as a function of pole radius for Redoubt and Spurr respectively. From the visual inspection, it can be seen that seismic energy increases with increasing pole radius, although the relation is not linear. In order to get a more complete view of the relationship between the pole radius and seismic energy, we divide the pole radius into quartile groups such as <25%, 25 to 50%, 50 to 75% and >75% and calculate their corresponding seismic energy, shown in the box-whisker plot in Fig. 6b and 6f. We have also estimated the average pole radius and seismic energy of these four groups and observed a linear relationship between them (i.e. the seismicity increases when the pole radius is large, Fig. 6c and 6g). Further, we compute the correlation coefficients between the PR and the seismic energy series as a function of the time lag and notice ~6–7 years' time lag between them (Fig. 6d and 6h). This time lag is similar to the 6.4-years periodicity of pole radius due to the beating between the Chandler and seasonal wobbles. The P_s value for both seismic energy and earthquakes associated with volcanoes are calculated following the same approach as in Section 3.1. From this analysis we observe that both seismic energy and earthquakes exhibit $P_s << 0.05$ values (inset in Fig. 6c and 6g), suggesting a statistical correlation with the polar motion at 95% confidence level.

In order to investigate whether volcanic activity preferentially occurs at specific phases of the polar motion cycle, we use circular linear correlation analysis (Mardia and Jupp, 2009). Volcanic activity times are converted into phase angles relative to the nearest peak of the polar radius cycle and the corresponding amplitudes of the polar radius are

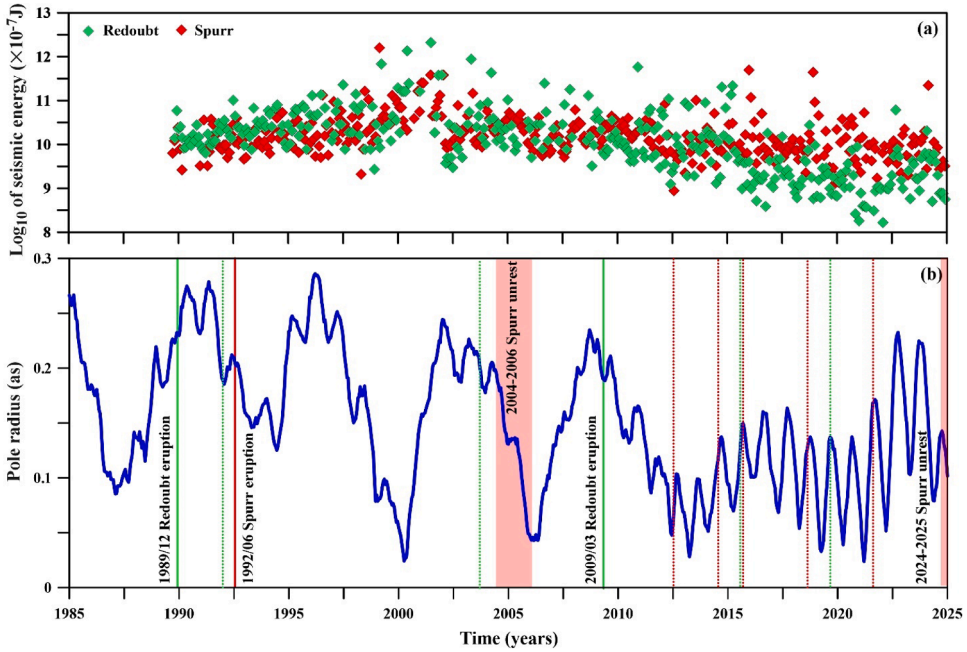

Fig. 5. (a) Monthly logarithm of seismic energy variation for the seismicity associated with Spurr and Redoubt volcano. (b) Time series of the pole radius in arc seconds for the same period as (a). The eruptions and non-eruptivity activity are represented by solid and dotted lines respectively. The unrest periods are indicated by red strips. Note that red color is for Spurr and green color for Redoubt volcano. Information related to the time of the eruptions and non-eruptivity activity is provided in Table S5.

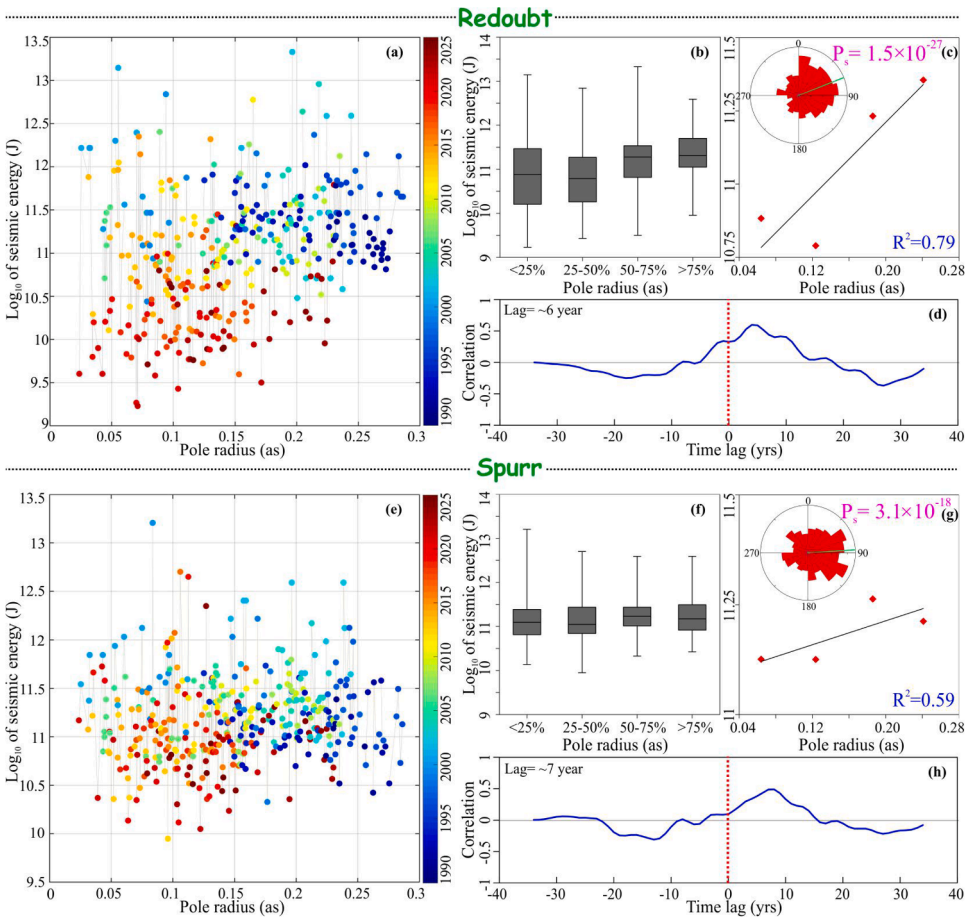

Fig. 6. (a and e) Relationship between mean of logarithm of seismic energy and pole radius for Spurr and Redoubt volcanoes respectively. (b, f) Box-Whisker plot for four classes of pole radius (i.e. < 25%, 25–50%, 50–75% and >75%) and corresponding logarithm of seismic energy. (c, g) Mean of four classes of pole radius versus logarithm of seismic energy. Insets show the polar plot of seismicity phase angles with respect to pole radius and Ps values shown in purple color. (d, h) Lag cross-correlation between the pole radius and seismicity. Note that there is a 6–7-year phase lag between the pole radius and seismicity.

obtained by linear interpolation. Due to the relatively small number of events, statistical significance is evaluated using a Monte Carlo permutation test with 10,000 random amplitude permutations while keeping phase angles fixed. The empirical p-value is calculated as the fraction of randomized datasets yielding a correlation coefficient equal to or greater than the observed value. We find a moderate correlation between volcanic activity phases and polar radius amplitude ($r \approx 0.417$), with an empirical p-value of ~0.028 (< 0.05), thus we can reject the null hypothesis of no correlation at the 95% confidence level (Fig. S11). This indicates a moderate, but statistically significant association between volcanic activity and polar motion and suggests that volcanic activities preferentially occur near specific phases of the polar radius cycle rather than being uniformly distributed throughout the cycle.

4. Influence of the tides on seismicity modulation

The Aleutian arc volcanoes are located close to the coast of the Pacific Ocean (Fig. 1), so it is reasonable to suggest that the tidal loading might be influencing the seismicity in this region. Therefore, we explore the tidal modulation of seismicity by performing power spectra analysis, using the same approach as in Section 3.1. From this analysis, we observe that the seismicity associated with the Aleutian Arc volcanoes does not exhibit any peak related to tidal periods (Fig. 7). Further, we also correlated the tidal load induced stress with seismicity occurrence. Here, we have calculated the total tidal stress (solid Earth tide + Ocean tide) at each Aleutian arc volcano center by using the SPOTL software (Agnew 1997, 2012). The tidal strains are calculated precisely by estimating Green's functions based on the Gutenberg-Bullen velocity model (Farrell, 1972) and an elastic and spherical Earth model (for details see supporting information). The estimated tidal strains are converted to tidal stress by adopting a linear elastic constitutive equation following Lambert et al. (2009) and considering an elastic modulus of 30 GPa and a Poisson ratio of 0.25. An example of a time series of horizontal and shear stresses induced by tidal loading are shown in Figure S12. After that, we calculate the P_s value by defining the phase angle of each earthquake occurrence with respect to the horizontal and shear tidal stress (see Section 3.1). The observed P_s values for all Aleutian volcanoes are > 0.05 except from Spurr (Table 1). Although, Ps value for the Spurr volcano is < 0.05, no prominent peak related to tides is observed in its spectrum (Fig. 7). This indicates that the correlation between the seismicity and tidal induced stress does not appear to be statistically significant (at 95% confidence) for the volcanoes included in this study.

5. Discussion

5.1. Effect of declustering on the results

Declustering is essential for isolating background seismicity by removing short-term dependent events that can bias periodicity patterns (Ader and Avouac, 2013). Several previous studies have employed declustered catalogs for analyzing seismicity modulation in volcano-tectonic environments, including Petrosino et al. (2018) at Campi Flegrei caldera; Sahoo et al. (2022) at Mount Etna; Miguelsanz

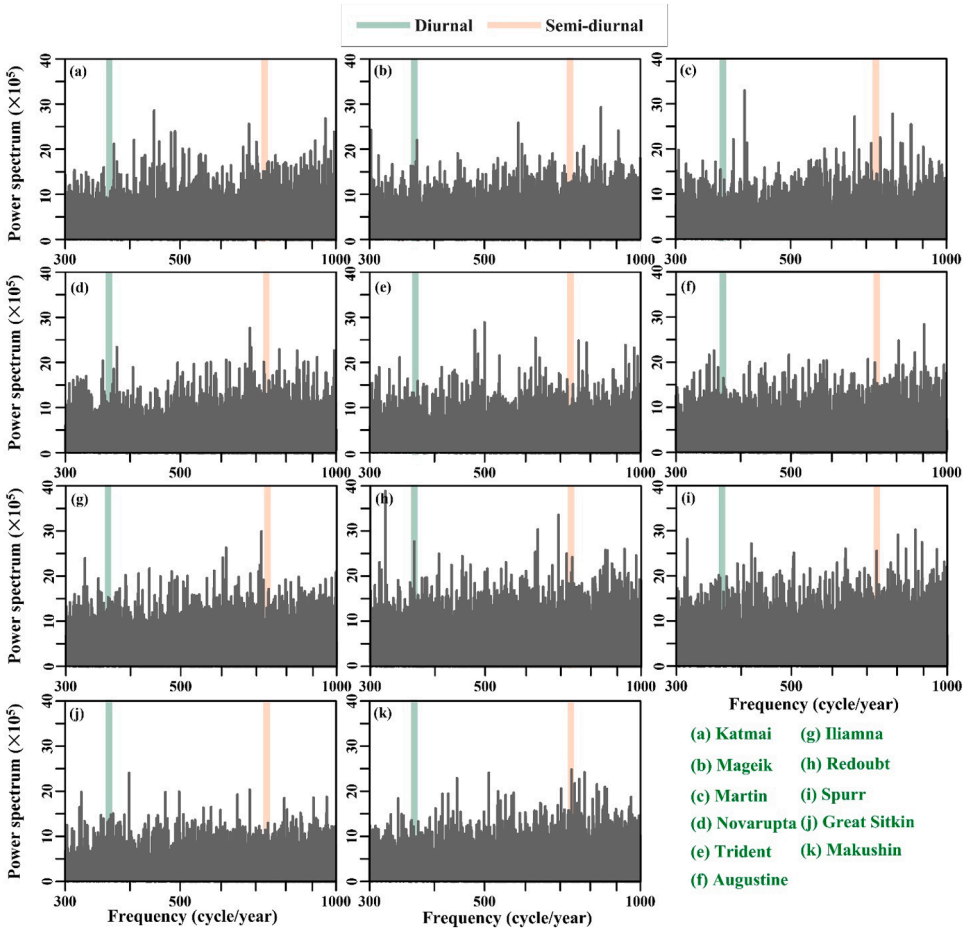

Fig. 7. Power spectra of declustered seismicity where the x-axis represents tidal frequency (cycle per year). The peach and green color strips indicate diurnal and semi-diurnal periodicity. Note that there is no evidence of tidal periodicity in any of the eleven volcanoes studied.

et al. (2023) at La Palma; Miguelsanz et al. (2021) at El Hierro; Lordi et al. (2022) in the Azores volcanic archipelago and Sahoo et al. (2021) at the Juan de Fuca Ridge. These studies indicate that declustering is considered in the published literature as a standard and essential step for analyzing seismicity modulation by external forcings. However, one could still argue that declustering may also obscure or amplify certain periodicities in the data.

To further evaluate the influence of declustering, we examine periodicity patterns using the full catalog above Mc (i.e., without applying declustering). We find that the power spectrum exhibits a strong exponential decay, which is characteristic of clustered seismicity dominated by aftershocks and short-term swarms. At KVG, spectral peaks similar to those in the declustered catalogs are still visible. In contrast, at CVG, although peaks related to annual, pole-tide, and pole-wobble periodicities remain present and are consistent with those from the declustered Mc catalogs, the high-frequency power from clustering partially obscures annual, pole-tide signals, making their interpretation less clear and more uncertain (Fig. S13). In order to get a clear view, we also examined the correlation between external forcings and the complete Mc catalogs (Figs. S14-S17). We found that some volcanoes (Katmai, Mageik, Novarupta, Trident and Great Sitkin) overall correlation between seismicity and snow load is broadly similar to those observed from declustered catalogs (Fig. S14-S15). However, for other volcanoes (Iliamna, Redoubt, Spurr, Makushin, Augustine and Martin), the correlations differ from the declustered results, mainly because of the high frequency (short-period) noise due to clustering (Figs. S14-S15). Similarly, correlations with pole-tide stress and polar motion radius also show similar trends to those observed in the declustered catalogs (Figs. S16-S17). The Ps values for several volcanoes decreased substantially (~2–20 times) when using the complete catalogs compared to the declustered catalogs (Table S4). This suggests that the presence of sudden burst events in the complete catalog may artificially influence Ps values and increase the correlation between the external forcing and seismicity.

An additional hypothesis, related to declustering, is that a combination of mainshock-aftershocks and swarms may be responsible for the periodicities we observe. In order to check this, we generate synthetic earthquake catalogs for each volcano that incorporate background seismicity, mainshock–aftershock sequences, and swarm activity within an Epidemic-Type Aftershock Sequence (ETAS) framework (see Text S3). In this approach, background events follow a homogeneous Poisson process, aftershock sequences are governed by magnitude-dependent productivity and Omori-type temporal decay, and swarm activity is represented by transient increases in seismicity rate independent of any single mainshock. To assess the statistical significance of the spectral features, we generate 1000 independent synthetic catalogs for each volcano comprising a combination of random mainshock-aftershocks and swarms using identical model parameters. The power spectrum of each catalog is then computed using the Fast Fourier Transform. At each frequency, the ensemble mean power and standard deviation are estimated, and the 95% confidence level was defined as the mean spectral power plus 1.96 times its standard deviation, assuming an approximately normal distribution of spectral power (see supporting information for details). The resulting power spectra of the synthetic catalogs do not exhibit significant periodicities (Fig. S18). This indicates that the periodic signals observed in the declustered catalogs cannot be

explained by a combination of random background seismicity, earthquake triggering, or swarm clustering alone, but instead reflect genuine temporal modulation of seismicity, likely associated with external forcing mechanisms.

5.2. Driving mechanisms for volcano seismicity modulation

We find that the snow load induced stress plays an important role in modulating seismicity for KVG volcanoes (Figs. 3–4). The rate of seismicity increases with decreasing snow load except from Martin volcano (Fig. 3). Similar results were also observed by researchers in Japan (Heki, 2003), California (Johnson et al., 2017) and western United States volcanic centers (Christiansen et al., 2005). The rate of seismicity in Katmai, Mageik, Novarupta and Trident is correlated with the negative vertical stress, while seismicity at Martin volcano is correlated with the peak vertical stress (Fig. S7). However, the seismicity rate is not increasing instantaneously with the peak or trough of vertical stress, which indicates that other factors may also be important such as pore fluid pressure, crack/fracture response to stress, viscoelastic behavior of the crust, and ability of the fluid to migrate through cracks (Martin and Durham, 1975; Beeler and Lockner, 2003). Here, we suggest two possible mechanisms to explain such seasonal modulation of seismicity in the KVG region. First, surficial loading-unloading (snow load) induces elastic stress-strain perturbations in the Earth's crust, leading to seasonal modulation of seismicity. Second, during the summer season, meltwater migrates to seismogenic depths along cracks, fractures and interconnected pore space of the upper-crustal rocks, resulting in an increase in pore fluid pressure. The elevated pore fluid pressure increases the Coulomb failure stress by reducing the effective normal stress at seismogenic depths, leading to a modulation of seismicity.

Furthermore, we find a weak correlation between seismicity and snow load induced stress in the CVG volcanoes (Figs. 2–4). This is probably due to the occurrence of more frequent eruptions and non-eruptive activities in this group (Fig. S2). A similar trend in seismicity modulation was observed during the 2015 Axial Seamount eruption on the Juan de Fuca Ridge (Wilcock, 2001; Sahoo et al., 2021). These studies reported a strong semi-diurnal tidal periodicity in the pre-eruption phase, which became weaker during the post-eruption period. It was suggested that volcano-tectonic processes likely dominated during the syn- and post-eruption phases, thereby masking the modulation of seismicity by tidal forces. Therefore, we also suggest that the volcano-tectonic forces in this region are several times higher than the external forcing, hence they dominate over the external snow loading stress and mask any seismicity modulation. In the case of Great Sitkin and Makushin volcano seismicity, we do not find any correlation with the snow load vertical stress, probably due to the small quantity of snow fall in these regions. This quantity is nearly ~4–5 times smaller than that observed in KVG and CVG regions (Fig. 3), which might not be sufficient to modulate the seismicity.

In some Aleutian volcanoes, we also find a strong correlation between seismic energy release from volcanoes and the polar motion, where both the number of earthquakes and seismic energy increase during periods of excursions of the Earth's rotation pole (Fig. 5& 6). Some recent studies also observed the crustal deformation and seismicity modulation due to the polar motion (Shen et al., 2005; Lambert and Sottili, 2019). The stress induced from the polar motion is in the order of less than ~1 kPa, which is much smaller than the interseismic stress (Mazzoti andAdams, 2004), but it may potentially trigger earthquakes in critically stressed volcanic and fault systems (Shen et al., 2005). Moreover, the mechanisms of earthquake modulation are very complex due to the interaction of various internal and external processes on a wide spatiotemporal scale. The effect of seismicity modulation strongly depends upon the oscillation period of external stress. Laboratory experiments and numerical modeling studies suggested that seismicity modulation can occur only when the period of external stress perturbations is either shorter or significantly longer than the earthquake nucleation periods (Beeler and Lockner, 2003; Ader et al., 2014). Beeler and Lockner (2003) also proposed that seismicity can be influenced by external loading when the loading amplitude is an order of magnitude smaller than the accumulated tectonic stress during a single cycle. They further noted that the minimum nucleation period for earthquakes on major active faults is approximately one year. This suggests that the triggering threshold for intermediate to longer external periodic loading (i.e. annual to interannual) could be much lower than the shorter external periodic loading (hour to days). In the present study, we observe that the seismicity rate increases during the time of hydrological unloading and periods of excursions of the Earth's rotation pole. This suggests that the annual hydrological cycle as well as the interannual Earth polar motion cycle are comparable to the earthquake nucleation time in the Aleutian arc volcanic center region. Hence, the snow load and polar motion induced stress may be capable of modulating the seismicity in the Aleutian arc volcanic centers, whereas diurnal and semi-diurnal Earth tides are not. Although the tidal modulation was observed to influence the occurrence of slow slip events and tectonic tremors, such seismic sources might have different frictional properties than the volcanic and conventional earthquakes (Beeler et al., 2018).

5.3. Influence of volcanic unrest and seismogenic depth on seismicity modulation

External periodic forcings do not influence all volcanic systems uniformly. Their effect depends on both the state of the volcano and the depth of seismicity. During the period of volcanic unrest, elevated pressure within the magma system weakens the surrounding crust, bringing the fault system closer to failure and increasing its sensitivity to small external stress perturbations (Miguelsanz et al., 2021). In order to investigate whether volcanic unrest influences the seismicity modulation, we identify documented unrest intervals of the volcanoes considered in the present study. During our analysis, we found four representative examples of volcanoes (Trident, Augustine, Spurr, and Makushin) that experienced episodes of unrest. We then remove all seismic events associated with these intervals and examine the spectral analysis on the modified catalogs (Fig. S19). We find that the power spectra exhibit nearly the same dominant periodicities as those observed from the declustered Mc catalog. This suggests that volcanic unrest likely does not have a measurable influence on the modulation of seismicity due to its relatively short duration. Therefore, the seismicity modulation patterns observed in this study appear to be independent of short-term volcanic activity.

Similarly, seismogenic depth may also be related to seismicity modulation, as surface-driven stresses from hydrological loading, tides, and rotational forcing decay rapidly with depth, making shallow earthquakes far more responsive to these variations than deeper events. Some volcanic centers considered in this study exhibit very shallow seismicity (<3 km), while others exhibit deeper activity, such as Iliamna (7 km), Redoubt (8 km), Spurr (10 km), Great Sitkin (6 km), and Makushin (12 km). However, not all of these volcanoes are suitable for depth-dependent periodicity analysis. In the case of Iliamna and Great Sitkin, the majority of earthquakes clusters are located above 4 km. Therefore, only three volcanoes (Redoubt, Makushin and Spurr) provide enough events for depth-dependent analysis. We divided seismicity into shallow (<5 km) and deeper (>5 km) groups to ensure that each subset contained enough events for spectral analysis. The results show that the spectral peaks corresponding to external forcing decrease with depth (Fig. S20). Geophysical studies indicate that magma storage zones are located at Makushin (~6–12 km), Redoubt (~4–9 km), and Spurr (~10–40 km) (Koulakov et al., 2013; Kasatkina et al., 2014; Lanza et al., 2022), and may affect the deeper seismicity. This suggests that external forcings predominantly modulate shallow seismicity in the Aleutian volcanic arc, whereas deeper earthquakes exhibit weak modulation, either because the external stress perturbations attenuate with depth or

more likely because they are related to the magmatic system of each volcano

5.4. Background stress level and critical triggering threshold

The threshold value of external stress perturbations and background stress level are also very important in order to understand the modulation of seismicity. The background stress rate is expressed as (Turcotte and Schubert, 2002)

$$\dot{\sigma} = \mu \frac{v}{d} \tag{9}$$

where $\dot{\sigma}$ is stress rate, μ is shear modulus of crust, v is the long-term plate velocity and d is the locking depth. Considering μ=30 GPa, $v = 65$mm/yr (Cross and Freymueller, 2008) and $d = 20$–30 km (Ohta et al., 2006), we estimate that the background stress rate at the Aleutian region is about 50–100 kPa/yr. Then, we use the elastic half-space solution of Boussinesq for considering a uniformly loaded circular disk to quantify surface mass variations stress at seismogenic depths, which is expressed as (Jager et al., 2007)

$$\sigma_z = \sigma\left[1 - \left(1 + \left(\frac{a}{z}\right)^2\right)^{-1.5}\right] \tag{10}$$

where σ_z is the stress at depth, σ is the stress at surface, α is the disk of radius and z is the depth. We estimate that surface loading from snow can produce stress changes on the order of 0.85–1.90 kPa and 2.0–2.80 kPa at the seismogenic depths of the Katmai volcanic group and the Cook Inlet group respectively. In comparison, pole tide stress contributes smaller stress variations of 0.2–0.3 kPa at these depths. Although the estimated surface load is much less compared to the tectonic background stress rate, it is comparable with the previously reported surface loading stress in various tectonic settings worldwide (Heki, 2003; Shen et al., 2005; Craig et al., 2017; Johnson et al., 2017; Ueda et al., 2024 etc.). Further, Ziv and Rubin (2000) investigated the lower threshold value of external stress perturbation for earthquake triggering and suggested that there is no such threshold in central California. Hence, when a fault or volcanic system is critically stressed, even a small variation in external stress may destabilize the system and modulate seismicity (Perfettini et al., 2001).

5.5. Impact of external forcing on seismicity and volcanic activity

The modulation of volcanic and seismic activity across seasonal to multi-year timescales indicate a potential sensitivity of the Earth's lithosphere to external forcing mechanisms (Heki, 2003; Craig et al., 2017; Lambert and Sottili, 2019; Senapati et al., 2024). In this study, we investigated the potential roles of climate-driven mass redistribution and rotational variations of the Earth in modulating seismic and volcanic activity (Fig. 3, 5b and S21). We find that eruptions, non-eruptive activity and unrest periods at Spurr and Redoubt volcanoes predominantly coincide with the largest excursions of the Earth's rotational pole (Fig. 5b). The observed correlation between polar motion amplitude, seismicity and volcanic activity suggests a plausible dynamic coupling between surface processes and deep Earth responses. This supports earlier findings by Lambert and Sottili (2019), who argued that long-period changes in the Earth's rotation could act as a modulator of volcanic unrest through stress transfer mechanisms. Further, our analysis also reveals a clear seasonal modulation of volcanic activity (Fig. S21). Non-eruptive activity at KVG increases during the winter months, coinciding with maximum hydrological loading (Fig. S21a). This behavior suggests that snow and associated surface loads modulate subsurface stress and promote non-eruptive activity (Heki, 2003). In contrast, eruptions, non-eruptive activity and unrest periods at CVG display the opposite seasonal trend, with enhanced activity during the summer months (Fig. S21b). This suggests that hydrological unloading, rather than loading, may play a dominant role in modulating seismicity in this region, potentially reflecting differences in crustal permeability, magma storage depth, or fault orientation relative to the applied seasonal stress (Amos et al., 2014). Eruptions and non-eruptive activity at Great Sitkin and Makushin, as well as the combined dataset of all three volcanic groups, shows no statistically significant correlation with external forcings (Fig. S21c–d). The absence of a coherent seasonal signal at these sites may indicate that the stress perturbations from hydrological or climatic loading are too small relative to background tectonic stresses, or that local crustal conditions prevent effective stress transfer (Bettinelli et al., 2008). These contrasting responses highlight that the influence of external forcings on volcanic systems is highly site-specific and controlled by a combination of crustal diffusivity, hydrological regime, and volcanic plumbing geometry (Singer et al., 2024).

Variations in surface loads due to snow accumulation and melt, glacial mass changes, groundwater fluctuations, atmospheric pressure and the variation in the Earth's rotational parameters can induce transient elastic and poroelastic deformation (Bürgmann et al., 2024). These processes affect effective normal stress on faults and influence fluid migration within magmatic and hydrothermal systems. In volcanic regions, such seasonal stress perturbations can modify the permeability of fracture networks, promote degassing, and potentially trigger shallow seismicity. The response of volcanic systems to external forcing is highly variable and depends on local geological and tectonic conditions, including magma composition, reservoir depth, fault orientation, and crustal permeability. While external forcing may not initiate volcanic unrest or earthquakes independently, it may act as a modulating or triggering factor in systems that are already near failure thresholds (Perfettini et al., 2001; Senapati et al., 2023). In addition to external forcing, internal volcanic processes (i.e., magma-chamber pressurization, volatile exsolution and fluid migration etc.) can also influence seismicity. Although such processes can generate their own cycles, they would not be expected to produce periodicities that match the frequencies of external forcings, nor the consistent phase alignment observed with snow-load and pole-tide cycles. The close correspondence between the observed spectral peaks and the known periods of these external forcings along with their physical plausibility, provides strong evidence that external processes contribute meaningfully to seismicity modulation. Finally, we suggest that periodic oscillation of external forcing acting on volcanic systems can change the state of the stress conditions in the crust, potentially influencing the timing and magnitude of earthquakes and volcanic eruptions. Therefore, the study of sensitivity of magmatic systems to periodic loading may help to understand their dynamics and even improve volcanic eruption forecasts.

6. Conclusions

This study explored the influence of periodic external forcings on volcanic seismicity along the Aleutian arc using earthquake catalogs spanning almost three decades. Our results indicate that climate-driven mass redistribution such as seasonal snow loading and variations in the Earth's rotational dynamics may influence the modulation of volcano seismicity. Based on the quantitative analysis of seismicity and its correlation with periodic external forcings, we draw the following key conclusions:

- We observe strong seasonal modulation of seismicity at KVG, weaker modulation at CVG, and no seasonal modulation at Great Sitkin and Makushin volcanoes. This result is strongly correlated with the snow depth variation, hence peak seismicity occurs during hydrological unloading periods. Notably, Seismicity exhibits 2–3 months' phase lag with hydrological loading, reflecting the time required for meltwater to migrate to seismogenic depths. Hence, we suggest that meltwater percolates through cracks, fractures, and interconnected pore spaces of the upper crust, resulting in an increase in pore fluid

pressure. This high pore fluid pressure increases the Coulomb failure stress by reducing effective normal stress, leading to a modulating seismicity.

- Seismicity associated with Augustine, Iliamna, Novarupta and Martin volcanoes exhibits 14-months periodicity, whereas the seismicity associated with Spurr and Redoubt volcanoes shows 6.4-year periodicity. These seismicity modulations are related to centrifugal forces due to changes in the Earth's rotation rate and in the direction of its rotation axis. However, we have not observed any significant seismicity modulation along the volcanoes included in this study that could be related to the Earth or Ocean tides.
- We find a moderate but statistically significant correlation between volcanic activity and polar radius amplitude. Specifically, volcanic activity at Spurr and Redoubt volcanoes occurs near the peaks of the pole radius, indicating that variations in the Earth's rotation rate and polar motion modulate stress within these volcanic systems and may influence the timing of volcanic activity.

Data availability

The data used in the present study are archived from the relevant public domains. The AVO catalog (1989–2024) used in this study for the period 1989–2017 is provided in the electronic supplement of Power et al. (2019), while data for 2018–2024 can be accessed through the United States Geological Survey (USGS) website: https://earthquake.usgs.gov/earthquakes/search/. The snow depth data is available at https://giovanni.gsfc.nasa.gov/giovanni/. The polar motion data is available at the International Earth Rotation and Reference System Service Earth Orientation Centre (https://www.iers.org/IERS/EN/DataProducts/EarthOrientationData/eop.html). Information related to the time of the eruptions and related phenomena for each volcano was adopted from the Alaska Volcano Observatory (https://avo.alaska.edu/explore/eruptions). All other material can be obtained from the corresponding author upon reasonable request.

CRediT authorship contribution statement

B. Senapati: Writing – review & editing, Writing – original draft, Visualization, Validation, Software, Methodology, Investigation, Formal analysis, Conceptualization. **K.I. Konstantinou:** Writing – review & editing, Visualization, Validation, Supervision, Project administration, Conceptualization.

Declaration of competing interest

The authors declare that they have no known competing financial interests or personal relationships that could have appeared to influence the work reported in this paper.

Acknowledgments

This research has been supported by a grant awarded to K.I.K by National Science and Technology Council (NSTC), Taiwan. B.S. is supported by the NSTC, Taiwan Postdoctoral fellowship. We thank the editor Carolina Lithgow-Bertelloni and two anonymous reviewers for their constructive comments, which improved the quality of the manuscript.

Supplementary materials

Supplementary material associated with this article can be found, in the online version, at doi:10.1016/j.epsl.2026.120025.

References

Ader, T.J., Lapusta, N., Avouac, J.P., Ampuero, J.P., 2014. Response of rate-and-state seismogenic faults to harmonic shear-stress perturbations. Geophys J Int 198 (1), 385–413. https://doi.org/10.1093/gji/ggu144.

Ader, T.J., Avouac, J.P., 2013. Detecting periodicities and declustering in earthquake catalogs using the Schuster spectrum, application to himalayan seismicity. Earth Planet. Sci. Lett. 377, 97–105. https://doi.org/10.1016/j.epsl.2013.06.032.

Agnew, D., 1997. NLOADF: a program for computing ocean-tide loading. J. Geophys. Res. 5109–5110. https://doi.org/10.1029/96JB03458.

Agnew, D.C., 2012. SPOTL: Some Programs For Ocean-Tide Loading. Scripps Institution of Oceanography, San Diego. UCRetrieved from. https://escholarship.org/uc/item/954322pg.

Alparone, S., Maiolino, V., Mostaccio, A., Scaltrito, A., Ursino, A., Barberi, G., et al., 2015. Instrumental seismic catalogue of Mount Etna earthquakes (Sicily, Italy): ten years (2000–2010) of instrumental recordings. Annals of Geophysics 58, S0435. https://doi.org/10.4401/ag-6591.

Amos, C.B., Audet, P., Hammond, W.C., Bürgmann, R., Johanson, I.A., Blewitt, G., 2014. Uplift and seismicity driven by groundwater depletion in central California. Nature 509 (7501), 483–486. https://doi.org/10.1038/nature13275.

Beeler, N.M., Lockner, D.A., 2003. Why earthquakes correlate weakly with the solid Earth tides: effects of periodic stress on the rate and probability of earthquake occurrence. Journal of Geophysical Research: Solid Earth 108 (B8). https://doi.org/10.1029/2001JB001518.

Beeler, N.M., Thomas, A., Bürgmann, R., Shelly, D., 2018. Constraints on friction, dilatancy, diffusivity, and effective stress from low-frequency earthquake rates on the deep San Andreas Fault. Journal of Geophysical Research: Solid Earth 123 (1), 583–605. https://doi.org/10.1002/2017JB015052.

Bettinelli, P., Avouac, J.P., Flouzat, M., Bollinger, L., Ramillien, G., Rajaure, S., Sapkota, S., 2008. Seasonal variations of seismicity and geodetic strain in the Himalaya induced by surface hydrology. Earth Planet. Sci. Lett. 266 (3–4), 332–344. https://doi.org/10.1016/j.epsl.2007.11.021.

Bizouard, C., Lambert, S., Gattano, C., Becker, O., Richard, J.Y., 2019. The IERS EOP 14C04 solution for Earth orientation parameters consistent with ITRF 2014. J. Geod. 93 (5), 621–633. https://doi.org/10.1007/s00190-018-1186-3.

Boettcher, M.S., Marone, C.J., 2004. Effects of normal stress variation on the strength and stability of creeping faults. J. Geophys. Res. 109, B03406. https://doi.org/10.1029/2003JB002824.

Bürgmann, R., Chanard, K., Fu, Y., 2024. Climate-and weather-driven solid Earth deformation and seismicity. GNSS Monitoring of the Terrestrial Environment. Elsevier, pp. 257–285. https://doi.org/10.1016/B978-0-323-95507-2.00011-6.

Buurman, H., Nye, C.J., West, M.E., Cameron, C., 2014. Regional controls on volcano seismicity along the Aleutian arc. Geochemistry, Geophysics, Geosystems 15 (4), 1147–1163. https://doi.org/10.1002/2013GC005101.

Christiansen, L.B., Hurwitz, S., Saar, M.O., Ingebritsen, S.E., Hsieh, P.A., 2005. Seasonal seismicity at western United States volcanic centers. Earth Planet. Sci. Lett. 240 (2), 307–321. https://doi.org/10.1016/j.epsl.2005.09.012.

Craig, T.J., Chanard, K., Calais, E., 2017. Hydrologically-driven crustal stresses and seismicity in the New Madrid seismic Zone. Nat Commun 8 (1), 2143. https://doi.org/10.1038/s41467-017-01696-w.

Cross, R.S., Freymueller, J.T., 2008. Evidence for and implications of a Bering plate based on geodetic measurements from the Aleutians and western Alaska. Journal of Geophysical Research: Solid Earth 113 (B7). https://doi.org/10.1029/2007JB005136.

Dzurisin, D., 1980. Influence of fortnightly Earth tides at Kilauea Volcano, Hawaii. Geophys Res Lett 7 (11), 925–928. https://doi.org/10.1029/GL007i011p00925.

Farrell, W.E., 1972. Deformation of the Earth by surface loads. Review of Geophysics 10, 761. https://doi.org/10.1029/RG010i003p00761.

Fierstein, J., Hildreth, W., 1992. The plinian eruptions of 1912 at Novarupta, Katmai national park, Alaska. Bull Volcanol 54 (8), 646–684. https://doi.org/10.1007/BF00430778.

Girona, T., Huber, C., Caudron, C., 2018. Sensitivity to lunar cycles prior to the 2007 eruption of Ruapehu volcano. Sci Rep 8 (1), 1–9. https://doi.org/10.1038/s41598-018-19307-z.

Gross, R.S., 2000. The excitation of the Chandler wobble. Geophys Res Lett 27 (15), 2329–2332. https://doi.org/10.1029/2000GL011450.

Gutenberg, B., Richter, C.F., 1944. Frequency of earthquakes in California. Bulletin of the Seismological society of America 34 (4), 185–188.

Heki, K., 2003. Snow load and seasonal variation of earthquake occurrence in Japan. Earth Planet. Sci. Lett. 207, 159–164. https://doi.org/10.1016/S0012-821X(02)01148-2.

Jaeger, J.C., Cook, N.G.W., Zimmerman, R.W., 2007. Fundamentals of Rock Mechanics, 4th edition. Blackwell Publishing, Malden, Massachusetts, p. 475.

Jentzsch, G., Haase, O., Kroner, C., Winter, U., 2001. Mayon volcano, Philippines: some insight into stress balance. Journal of Volcanology and Geothermal Research 109 (1–3), 205–217. https://doi.org/10.1016/S0377-0273(00)00312-7.

Johnson, C.W., Fu, Y., Bürgmann, R., 2017. Seasonal water storage, stress modulation, and California seismicity. Science 356 (6343), 1161–1164. https://doi.org/10.1126/science.aak9547.

Kasahara, J., Nakao, S., Koketsu, K., 2001. Tidal influence on the 2000 Miyake-jima eruption and its implications for hydrothermal activity and volcanism. Proceedings Japan Academy 77 (6), 98–103. https://doi.org/10.2183/pjab.77.98.

Kasatkina, E., Koulakov, I., West, M., Izbekov, P., 2014. Seismic structure changes beneath Redoubt Volcano during the 2009 eruption inferred from local earthquake tomography. Journal of Geophysical Research: Solid Earth 119 (6), 4938–4954. https://doi.org/10.1002/2013JB010935.

Konstantinou, K.I., 2022. Multiyear temporal variation of b-values at Alaskan volcanoes: the synergetic influence of stress and material heterogeneity. Journal of Volcanology and Geothermal Research 427, 107572. https://doi.org/10.1016/j.jvolgeores.2022.107572.

Koulakov, I., West, M., Izbekov, P., 2013. Fluid ascent during the 2004–2005 unrest at Mt. Spurr inferred from seismic tomography. Geophys Res Lett 40 (17), 4579–4582. https://doi.org/10.1002/grl.50674.

Lanza, F., Roman, D.C., Power, J.A., Thurber, C.H., Hudson, T., 2022. Complex magmatic-tectonic interactions during the 2020 Makushin Volcano, Alaska, earthquake swarm. Earth Planet. Sci. Lett. 587, 117538. https://doi.org/10.1016/j.epsl.2022.117538.

Lambeck, K., 1980. The Earth's variable rotation: Geophysical causes and Consequences. Cambridge University Press, Cambridge.

Lambert, A., Kao, H., Rogers, G., Courtier, N., 2009. Correlation of tremor activity with tidal stress in the northern Cascadia subduction zone. Journal of Geophysical Research: Solid Earth 114, B00A08. https://doi.org/10.1029/2008JB006038.

Lambert, S., Sottili, G., 2019. Is there an influence of the pole tide on volcanism? Insights from Mount Etna recent activity. Geophys Res Lett 46 (23), 13730–13736. https://doi.org/10.1029/2019GL085525.

Lordi, A.L., Neves, M.C., Custódio, S., Dumont, S., 2022. Seasonal modulation of oceanic seismicity in the azores. Frontiers in Earth Science 10, 995401. https://doi.org/10.3389/feart.2022.995401.

Mardia, K.V., Jupp, P.E., 2009. Directional Statistics. John Wiley & Sons.

Martin III, R.J., Durham, W.B, 1975. Mechanisms of crack growth in quartz. J. Geophys. Res. 80 (35), 4837–4844. https://doi.org/10.1029/JB080i035p04837.

Mazzotti, S., Adams, J., 2004. Variability of near-term probability for the next great earthquake on the Cascadia subduction zone. Bulletin of the Seismological Society of America 94 (5), 1954–1959. https://doi.org/10.1785/012004032.

McNutt, S.R., Beavan, R.J., 1987. Eruptions of Pavlof volcano and their possible modulation by ocean load and tectonic stresses. Journal of Geophysical Research: Solid Earth 92 (B11), 11509–11523. https://doi.org/10.1029/JB092iB11p11509.

McNutt, S.R., Roman, D.C., 2015. Volcanic seismicity. The Encyclopedia of Volcanoes. Academic Press, pp. 1011–1034. https://doi.org/10.1016/B978-0-12-385938-9.00059-6.

Miguelsanz, L., Fernandez, J., Prieto, J.F., Tiampo, K.F., 2023. Tidal modulation of the seismic activity related to the 2021 La Palma volcanic eruption. Sci Rep 13 (1), 6485. https://doi.org/10.1038/s41598-023-33691-1.

Miguelsanz, L., González, P.J., Tiampo, K.F., Fernández, J., 2021. Tidal influence on seismic activity during the 2011–2013 El Hierro volcanic unrest. Tectonics 40 (2), e2020TC006201. https://doi.org/10.1029/2020TC006201.

Nakajima, J., Uchida, N., 2018. Repeated drainage from megathrusts during episodic slow slip. Nat Geosci 11 (5), 351–356. https://doi.org/10.1038/s41561-018-0090-z.

Ohta, Y., Freymueller, J.T., Hreinsdóttir, S., Suito, H., 2006. A large slow slip event and the depth of the seismogenic zone in the south central Alaska subduction zone. Earth Planet. Sci. Lett. 247 (1–2), 108–116. https://doi.org/10.1016/j.epsl.2006.05.013.

Perfettini, H., Schmittbuhl, J., Rice, J.R., Cocco, M., 2001. Frictional response induced by time-dependent fluctuations of the normal loading. Journal of Geophysical Research: Solid Earth 106 (B7), 13455–13472. https://doi.org/10.1029/2000JB900366.

Petit, G., Luzum, B., 2010. Conventions 2010. IERS Technical Note 36. Verlag des Bundesamts für Kartographie und Geodäsie, Frankfurt am Main, p. 179. ISBN: 3-89888-989-6.

Petrosino, S., Cusano, P., Madonia, P., 2018. Tidal and hydrological periodicities of seismicity reveal new risk scenarios at Campi Flegrei caldera. Sci Rep 8 (1), 13808. https://doi.org/10.1038/s41598-018-31760-4.

Power, J.A., Friberg, P.A., Haney, M.M., Parker, T., Stihler, S.D., Dixon, J.P., 2019. A unified catalog of earthquake hypocenters and magnitudes at volcanoes in Alaska-1989 to 2018. U. S. Geological Survey Scientific Investigations Report 2019-5037, 17. https://doi.org/10.3133/sir20195037.

Power, J.A., Haney, M.M., Botnik, S.M., Dixon, J.P., Fee, D., Kaufman, A.M., Ketner, D. M., Lyons, J.J., Parker, T., Paskievitch, J.F., Read, C.W., Searcy, C., Stihler, S.D., Tepp, G., Welch, A.G., 2020. Goals and development of the Alaska Volcano observatory seismic network and application to forecasting and detecting volcanic eruptions. Seismological Research Letters 91 (2), 647–659. https://doi.org/10.1785/0220190216.

Reasenberg, P., 1985. Second-order moment of central California seismicity, 1969–1982. Journal of Geophysical Research-Solid Earth 90 (B7), 5479–5495. https://doi.org/10.1029/JB090iB07p05479.

Saar, M.O., Manga, M., 2003. Seismicity induced by seasonal groundwater recharge at Mt. Hood, Oregon. Earth Planet. Sci. Lett. 214 (3–4), 605–618. https://doi.org/10.1016/S0012-821X(03)00418-7.

Sahoo, S., Senapati, B., Panda, D., Tiwari, D.K., Santosh, M., Kundu, B., 2021. Tidal triggering of micro-seismicity associated with caldera dynamics in the Juan de Fuca ridge. Journal of Volcanology and Geothermal Research 417, 107319. https://doi.org/10.1016/j.jvolgeores.2021.107319.

Sahoo, S., Tiwari, D.K., Panda, D., Kundu, B., 2022. Eruption cycles of Mount Etna triggered by seasonal climatic rainfall. J Geodyn 149, 101896. https://doi.org/10.1016/j.jog.2021.101896b.

Senapati, B., Kundu, B., Jin, S., 2022. Seismicity modulation by external stress perturbations in plate boundary vs. stable plate interior. Geoscience Frontiers 13 (3), 101352. https://doi.org/10.1016/j.gsf.2022.101352.

Senapati, B., Kundu, B., Jin, S., Santosh, M., 2024. Drought-induced seismicity modulation in the New Madrid Seismic Zone, central United States. Geosphere 20 (5), 1347–1363. https://doi.org/10.1130/GES02702.1.

Senapati, B., Kundu, B., Perfettini, H., Gahalaut, V.K., Singh, A.K., Ghosh, A., Rao, N.P., 2023. Fault resonance process and its implications on seismicity modulation on the active fault system. Tectonophysics 861, 229920. https://doi.org/10.1016/j.tecto.2023.229920.

Shen, Z.K., Wang, Q., Bürgmann, R., Wan, Y., Ning, J., 2005. Pole-tide modulation of slow slip events at circum-Pacific subduction zones. Bulletin of the Seismological Society of America 95 (5), 2009–2015. https://doi.org/10.1785/0120050020.

Singer, B.S., Moreno-Yaeger, P., Townsend, M., Huber, C., Cuzzone, J., Edwards, B.R., Amigo, Á., 2024. New perspectives on ice forcing in continental arc magma plumbing systems. Journal of *Volcanology and Geothermal Research* 455, 108187. https://doi.org/10.1016/j.jvolgeores.2024.108187.

Sottili, G., Palladino, D.M., 2012. Tidal modulation of eruptive activity at open-vent volcanoes: evidence from Stromboli, Italy. Terra Nova 24 (3), 233–237. https://doi.org/10.1111/j.1365-3121.2012.01059.

Syracuse, E.M., Abers, G.A., 2006. Global compilation of variations in slab depth beneath arc volcanoes and implications. Geochemistry, Geophysics, Geosystems 7 (5). https://doi.org/10.1029/2005GC001045.

Talwani, P., Chen, L., Gahalaut, K., 2007. Seismogenic permeability, ks. Journal of Geophysical Research: Solid Earth 112 (B7). https://doi.org/10.1029/2006JB004665.

Tang, C.C., Lin, L.C., Luo, Y., Liu, S., Xu, R., Lin, C.H., 2019. Possible earth-tide modulations of early aftershocks in southern Taiwan. Bulletin of the Seismological Society of America 109 (4), 1571–1577. https://doi.org/10.1785/0120170381.

Tibaldi, A., Bonali, F.L., 2017. Intra-arc and back-arc volcano-tectonics: magma pathways at holocene Alaska-aleutian volcanoes. Earth-Science Reviews 167, 1–26. https://doi.org/10.1016/j.earscirev.2017.02.004.

Townend, J., Zoback, M.D., 2000. How faulting keeps the crust strong. Geology 28 (5), 399–402. https://doi.org/10.1130/0091-7613(2000)28<399:HFKTCS>2.0.CO;2.

Trauth, M.H., 2007. Introduction to MATLAB. MATLAB® Recipes for Earth Sciences. Springer, Berlin, Heidelberg. https://doi.org/10.1007/978-3-540-72749-1_2.

Turcotte, D.L., Schubert, G., 2002. Geodynamics, 2nd edition. Cambridge University Press, Cambridge, UK, p. 456. https://doi.org/10.1017/CBO9780511807442.

Ueda, T., Kato, A., Johnson, C.W., Terakawa, T., 2024. Seasonal modulation of crustal seismicity in northeastern Japan driven by snow load. Journal of Geophysical Research: Solid Earth 129, e2023JB028217. https://doi.org/10.1029/2023JB028217.

Wei, S.S., Ruprecht, P., Gable, S.L., Huggins, E.G., Ruppert, N., Gao, L., Zhang, H., 2021. Along-strike variations in intermediate-depth seismicity and arc magmatism along the Alaska Peninsula. Earth Planet. Sci. Lett. 563, 116878. https://doi.org/10.1016/j.epsl.2021.116878.

Wiemer, S., 2001. A software package to analyze seismicity: ZMAP. Seismological Research Letters 72 (3), 373–382. https://doi.org/10.1785/gssrl.72.3.373.

Wilcock, W.S., 2001. Tidal triggering of microearthquakes on the Juan de Fuca Ridge. Geophys Res Lett 28 (20), 3999–4002. https://doi.org/10.1029/2001GL013370.

Woessner, J., Wiemer, S., 2005. Assessing the quality of earthquake catalogues: estimating the magnitude of completeness and its uncertainty. Bulletin of the Seismological Society of America 95 (2), 684–698. https://doi.org/10.1785/0120040007.

Zaliapin, I., Gabrielov, A., Keilis-Borok, V., Wong, H., 2008. Clustering analysis of seismicity and aftershock identification. Phys. Rev. Lett. 101 (1), 018501. https://doi.org/10.1103/PhysRevLett.101.018501.

Ziv, A., Rubin, A.M., 2000. Static stress transfer and earthquake triggering: no lower threshold in sight? Journal of Geophysical Research: Solid Earth 105 (B6), 13631–13642. https://doi.org/10.1029/2000JB900081.